JOURNAL OF PHYSICAL ORGANIC CHEMISTRY, VOL. 6, 445–464 (1993)

STRUCTURE, STABILIZATION ENERGIES AND CHEMICAL SHIFTS OF THE CYCLOBUTENYL CATION. DOES IT HAVE 'AROMATIC' HOMOCYCLOPROPENIUM ION CHARACTER? AN *AB INITIO* STUDY

STEFAN SIEBER AND PAUL v. R. SCHLEYER*

Institut für organische Chemie der Friedrich-Alexander Universität Erlangen-Nürnberg, Henkestr. 42, D-91054 Erlangen, Germany

ANDRÉ HENRY OTTO*

AUF – Adlershofer Umweltschutztechnik- und Forschungsgesellschaft mbH, Rudower Chaussee 5, D-12489 Berlin, Germany

JÜRGEN GAUSS

Lehrstuhl für Theoretische Chemie, Institut für Physikalische Chemie, Universität Karlsruhe, D-76128 Karlsruhe, Germany

AND

FELIX REICHEL AND DIETER CREMER

Theoretical Chemistry, University of Göteborg, Kemigården 3, S-41296 Göteborg, Sweden

The relatively high stability and the structure of the simplest homoaromatic carbocation, the cyclobutenyl cation 1, was established *ab initio* by using correlated wave functions at HF 6–31G*, MP2(full)/6–31G*, MP2(full)/6–311G and MP4(SDQ,full)/6-31G* geometries. The stability of 1 was estimated using homodesmotic and isodesmic reactions. The heat of formation of 1 was estimated to be 244 kcal mol^{-1} (1 kcal = 4·184 kJ). Chemical shift calculations were carried out at correlated levels and are in good agreement with the experimental values. At all levels of theory chemical shift calculations confirm the bent structure of 1. The MP4(SDTQ,fc)/6–311G**//MP2(full)/6–311G** + ZPE(MP2/(full)6–31G*), QCISD(T,fc)/6–31 + G*//MP2(full)/6–31G* + ZPE(MP2(full)/6–31G*) and MP4(SDQ,full)/6–31G*//MP4(SDQ,full)/6–31G* + ZPE(MP2(full)/6–31G*) ring inversion energies of 9·1, 9·3 and 9·0 kcal mol^{-1}, respectively, agree with experiment (8·4 ± 0·5 kcal mol^{-1}). Triplet electronic states are not competitive energetically. The homoaromatic character of the cyclobutenyl cation is shown by the nearly equal charges on C-1, C-2 and C-3, the considerable 1,3-bond order, the short 1·74 Å C-1—C-3 distance and the large stabilization energy relative to the allyl cation.**

INTRODUCTION

In contrast to the detailed information which has long been available for bi- and polycyclic hydrocarbons,[1] structural data (e.g. bond lengths and bond angles) of comparable quality and reliability on the corresponding carbocations are only of recent origin.[2] The cyclobutenyl cation is of special interest as the smallest homoaromatic species. Owing to its homoaromatic stabilization it can be generated, e.g., from bicyclobutane by abstraction of a hydride ion under superacid conditions.[3] The $AlCl_3$ complex of tetramethylcyclobutadiene could be identified as an intermediate of the trimerisation of but-2-yne in the presence of aluminium chloride to yield hexamethyl-Dewar-benzene. Its crystal structure[4] shows a non-planar homocyclopropenylium moiety with a puckering angle of 148·5° and a 1·78 Å 1,3-distance, indicating a significant transannular interaction in agreement with homoaromaticity.

Homoaromaticity[5] as a general concept was introduced in 1959 by Winstein.[6,7] It rationalizes the chemical behaviour and the observed unusual stability of systems in which a possible aromatic conjugation is interrupted by one or more sp^3-hybridized carbon atoms or other saturated groups. In these systems the influence of the insulating group is avoided by

* Author for correspondence.

0894–3230/93/080445–20$15.00

Received 15 January 1993
Revised 22 March 1993

additional 1,3-orbital interaction, closing the cyclic conjugation. According to Winstein a system is homoaromatic when it meets four requirements [other definitions were introduced later (cf. Ref. 5), but are more or less closely related to Winstein's definition]: (a) a 1,3-bond exists, closing the cyclic conjugation, (b) the 1,3-bond order is significantly greater than zero; (c) the orbital overlap of the participating p-orbitals at the centres involved is between pure π and pure σ character; and (d) the $(4n + 2)$ π-electrons are fully delocalized over the closed cycle which results. These requirements may be verified theoretically, e.g by Natural Population Analysis (NPA)[8] and by a topological analysis of the MP2(full)/6–31G* response density.[9] The present results on the homocyclopropenylium cation **1**, calibrated against the neutral bicyclobutane **2**, are compared with the results for the isoelectronic homodiboriranide anion[10] **3** and the homotropylium cation **4**.[11]

Olah and co-workers synthesized a series of cyclobutenyl cations and determined an $8 \cdot 4 \pm 0 \cdot 5$ kcal mol^{-1} ring inversion barrier (1 kcal = 4·184 kJ), termed the 'homoaromatization energy',[12] for the parent species **1**.[3b] Because of its relatively small size, **1** has often been studied theoretically, *ab initio*[13,14] and at lower levels of approximation, e.g. EHT,[15] CNDO/2[16] and MINDO/3.[17] MP2/6–31G* single-point calculations also were performed on the MNDO optimized geometry.[18] MNDO,[19] AM1[20] and PM3[21] are all inadequate as they erroneously give only one stationary point for **1** with a planar C_{2v} geometry. Only MINDO/3[22] gives a non-planar minimum. Modern *ab initio* methods using large, flexible basis sets and including electron correlation can be expected to give reliable results. Although Haddon and Raghavachari[23] carried out Møller–Plesset perturbation calculations up to the fourth order (cf. Tables 1 and 2), the computed inversion energies of **1** were still too high. Two reasons may be responsible: neglect of zero-point energy corrections and the use of geometries optimized at Hartree–Fock rather than correlated levels. (Haddon and Raghavachari also employed geometries, optimized at MP2/6–31G*, but only the carbon skeleton was optimized. This procedure has now been recognized to be unreliable.) An earlier IGLO computation of the NMR chemical shifts also suffered from the use of unrefined geometries.[14]

METHOD OF CALCULATION

Most of the calculations were performed with the Gaussian 80 and 90 systems of programs.[24] CADPAC 4.1[25] was used for the MP2(full)/6–31G* frequency calculations. The singlet states (**1a** and **1b**) were calculated at restricted Hartree–Fock (RHF) while the triplet (**1c**) was calculated at the unrestricted level (UHF). The geometries were taken from Ref. 23 or were optimized with 3–21G, 6–31G* and 6–311G** standard basis sets,[1e] at the Hartree–Fock, MP2 and MP4(SDQ)[26] level. All stationary points were characterized by diagonalization of the second-derivative matrix of the energy and determination of the number of negative eigenvalues at Hartree–Fock and correlated level using the 6–31G* basis set. Energies of HF 6–31G*, MP2(full)/6–31G* and MP2(full)/6–311G** optimized geometries were improved by Møller–Plesset perturbation calculations[27] up to fourth order. These calculations were performed using frozen core approximation (fc, only valence electrons are taken into account) and also all electrons (full). In addition to MPn, CID(fc)/6–31G*//6–31G* and QCISD(T,fc)/6–31 + G*//MP2(full)/6–31G* single-point calculations[28] were carried out for **1a** and **1b**. Zero-point energies were calculated with the HF 6–31G* and the MP2(full)/6–31G* frequencies (and geometries); scaling factors of 0·89 and 0·94,[1e] respectively, were employed.

The heat of formation of **1a** was estimated using several isodesmic and homodesmotic bond separation reactions and also the group equivalent approach of Ibrahim and Schleyer.[29] However, only HF/6–31G* and MP2(full)/6–31G* group equivalents are available, as are the reference structures employed in isodesmic and homodesmotic reactions. Hence, most of the evaluations were restricted to the HF/6–31G* and MP2(full)/6–31G* levels.

The semi-empirical calculations were carried out using the program VAMP 4.4[30] with the EF optimization procedure.[31]

NMR chemical shifts were computed with the IGLO procedure of Kutzelnigg and Schindler,[32] using the standard DZ and II basis sets (a comprehensive description of method, basis sets and a review on recent applications of the IGLO method can be found in Ref. 33). In addition, for a decisive calculation of NMR chemical shifts at a correlated level, the new GIAO-MP2 [or GIAO-MBPT(2)] method[34] [note that MP2 and MBPT(2) mean the same type of perturbation theory] as implemented in the ACES II program system[35,36] together with DZP and TZP basis sets[37] have been employed.

RESULTS AND DISCUSSION

Structures and energies

The total energies of the geometries considered are presented in Table 1. The three stationary points for the cation (singlet **1a** and **1b**, triplet **1c**), were characterized by the number of negative eigenvalues in the force constant matrix at HF/6–31G* and at MP2(full)/6–31G*. While **1b** (C_s) and **1c** (C_{2v}) are minima, one negative eigenvalue was found for **1a** (C_{2v}). Structures for **1a**, **1b** and **1c** at HF/6-31G*, MP2(full)/6–311G** and

Table 1. Total energies (– a.u.) and ZPEs (kcal mol^{-1})

Computation level	Species					
	1a (C_{2v})	ZPE	**1b** (C_s)	ZPE	**1c**[a] (C_{2v} triplet)	ZPE
Geometry: 3–21G						
HF/3–21G	153·15394		153·15485		153·09245	
HF/6–31G*	154·03396		154·03811		153·97177	
Geometry: 6–31G*		50·13		50·85		47·11
HF/6–31G*	154·03556[b]		154·04251[b]		153·97666	
MP2(fc)/6–31G*	154·50864		154·52575		154·41301	
MP3(fc)/6–31G*	154·53842		154·55287		154·45080	
MP4(SDTQ,fc)/6-31G*	154·56517		154·57966		154·47219	
MP2(full)/6–31G*	154·52760		154·54480		154·43170	
MP3(full)/6–31G*	154·55718		154·57171		154·46935	
MP4(SDTQ,full)/6–31G*	154·58406		154·59863		154·49082	
CID(fc)/6–31G*	154·54286		154·55754		—	
Geometry: MP2(full)/6–31G*		47·85		48·18		44·13
MP2(fc)/6–31G*	154·50964		154·52826		154·41426	
MP3(fc)/6–31G*	154·53926		154·55458		154·45169	
MP4(SDTQ,fc)/6–31G*	154·56672		154·58219		154·47361	
MP2(full)/6–31G*	154·52848		154·54735		154·43295	
MP3(full)/6–31G*	154·55791		154·57334		154·47024	
MP4(SDTQ,full)/6–31G*	154·58549		154·60109		154·49224	
MP2(fc)/6–31G**	154·54721		154·56590		—	
MP3(fc)/6–31G**	154·57905		154·59423		—	
MP4(SDTQ,fc)/6–31G**	154·60628		154·62154		—	
MP2(full)/6–31G**	154·56686		154·58570		—	
MP3(full)/6–31G**	154·59851		154·61381		—	
MP4(SDTQ,full)/6–31G**	154·62586		154·64126		—	
MP2(fc)/6–31+G*	154·51246[c]		154·53133[c]		—	
MP3(fc)/6–31+G*	154·54211[c]		154·55751[c]		—	
MP4(SDQ,fc)/6–31+G*	154·54817[c]		154·56303[c]		—	
QCISD(fc)/6–31+G*	154·55000[c]		154·56484[c]		—	
QCISD(T,fc)/6–31+G*	154·57119[c]		154·58657[c]		—	
Geometry: MP2(full)/6–311G**						
MP2(full)/6–311G**	154·66376		154·68221		—	
MP2(fc)/6–311G**	154·58898		154·60719		—	
MP3(fc)/6–311G**	154·62081		154·63539		—	
MP4(SDTQ,fc)/6–311G**	154·65103		154·66603		—	
Geometry: MP4(SDQ)/6–31G*						
MP4(SDQ,full)/6–311G**	154·56389		154·57882		—	
MP4(SDTQ,full)/6–311G**	154·58555		154·60116		—	

[a] $^3B_2$ electronic state. The spin projected energies are given.
[b] Taken from Ref. 23.
[c] M. Bühl, unpublished work.

MP4(SDQ)/6–31G* are shown in Figure 1 and compared with the structure of bicyclobutane **2**. Major differences are found between Hartree—Fock and correlated geometries, while MP2(full)/6–311G**, MP2(full)/6–31G* (not shown) and MP4(SDQ)/6–31G* geometries are nearly identical. The decreased 1,3-bond length and the increased 1,2-bond length in **1b** reflect the influence of electron correlation on the highly delocalized electronic structure. The relative energy of **1a** and **1b**, the ring inversion barrier (also termed homoaromatization energy)[12] is given in Table 2. The experimental[3b] value of 8·4 ± 0·5 kcal mol^{-1} is reproduced by *ab initio* calculations for both Hartree–Fock and correlated level geometries, provided the energy was computed using perturbation theory at least to the third order and by taking zero-point energy differences into account. MPn inversion barriers oscillate with the order, *n*, of perturbation theory applied: HF ($n = 1$) values are much too low since HF underestimates the stability of **1b**. MP2 is known to prefer biradical, stret-

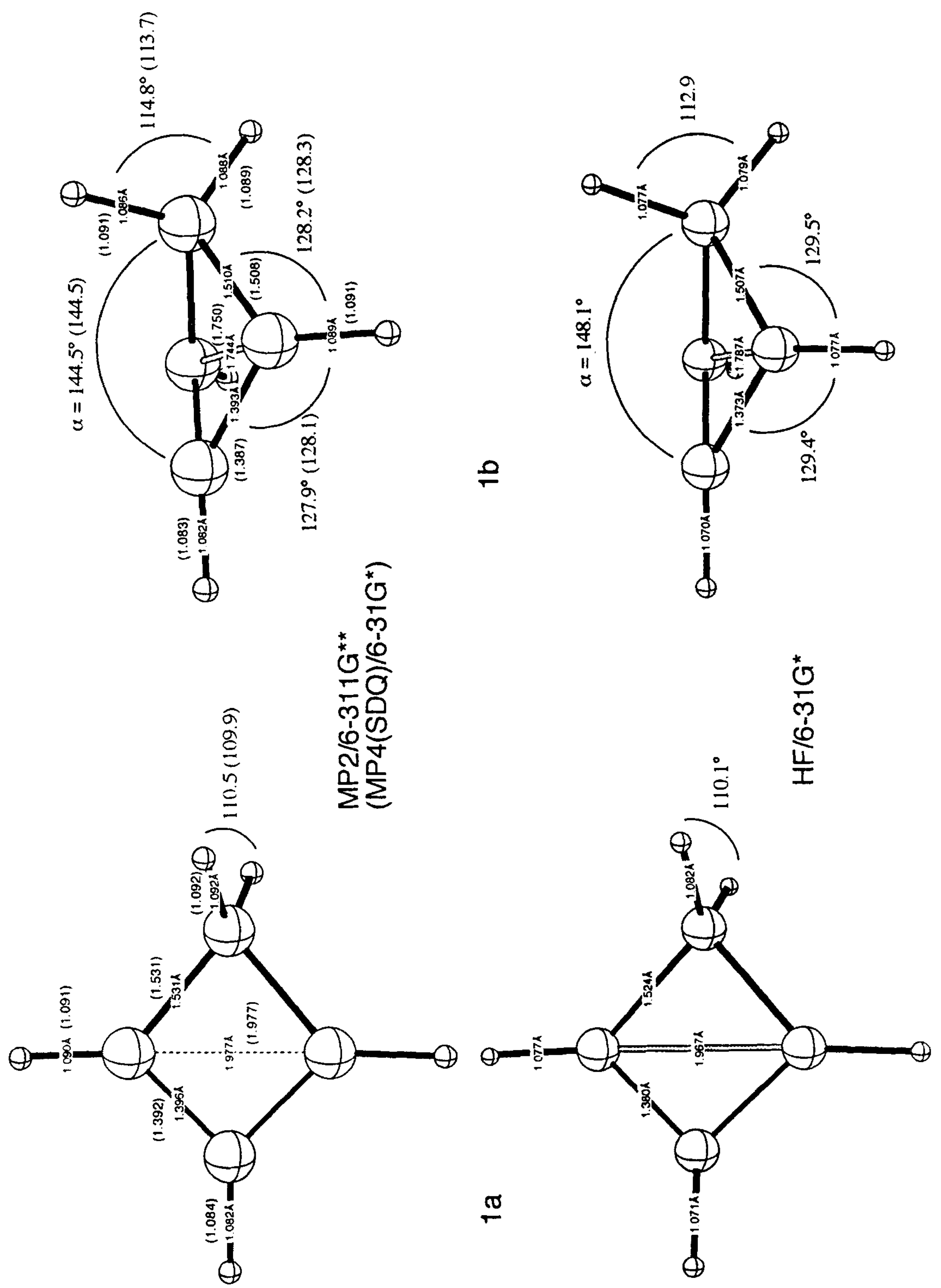
1a
1b
MP2/6-311G**
(MP4(SDQ)/6-31G*)
HF/6-31G*
α = 144.5° (144.5)
114.8° (113.7)
128.2° (128.3)
127.9° (128.1)
110.5 (109.9)
α = 148.1°
112.9
129.5°
129.4°
110.1°

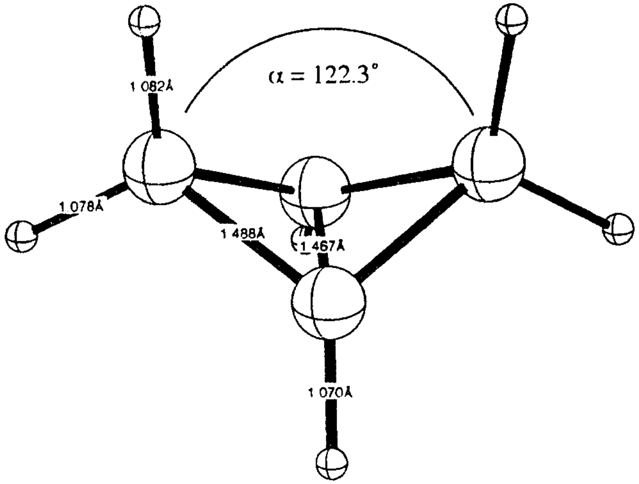

2

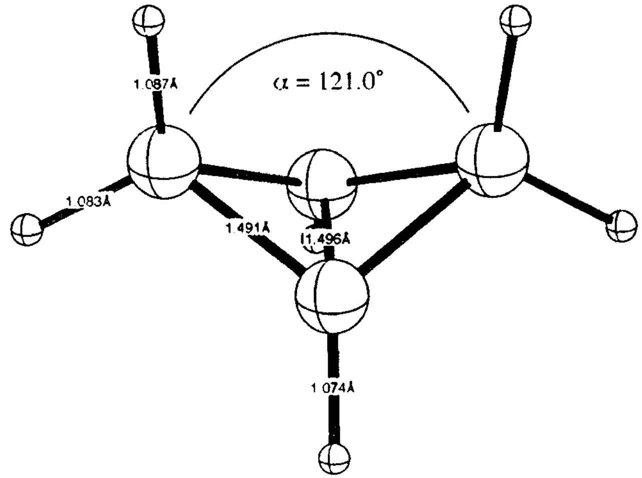

Figure 1. Calculated structures of the cyclobutenyl cation **1a** (C_{2v}), **1b** (C_s) and bicyclo[1.1.0]butane (**2**). HF/6–31G* and MP2(full)/6–311G** geometries are shown for comparison. MP2(full)/6–31G* geometries are nearly identical with the MP2(full)/6–311G** geometries (cf. Figure 4). Values in parentheses are for the MP4(SDQ)/6–31G* optimized structure

Table 2. Ring inversion (homoaromatization) energy (E_h) (kcal mol^{-1}) of the cyclobutenyl cation

Computational level	E_h	E_h including ZPE[a,b]
MINDO/3	9·8	
3-21G //3–21G	0·6	
4-31G//4–31G	0·7[c]	
6-31G//6–31G	0·8[c]	
6-31G*//3–21G	2·6	
6-31G*//6–31G*	4·4[c]	3·7[c]
MP2(fc)/6–31G*//6–31G*	10·7	10·1
MP2(full)/6–31G*//6–31G*	10·8	10·2
MP3(fc)/6–31G*//6–31G*	9·1	8·4
MP3(full)/6–31G*//6–31G*	9·1	8·4
MP4(SDTQ,fc)/6–31G*//6–31G*	9·1	8·4
MP4(SDTQ,full)/6–31G*//6–31G*	9·1	8·4
CID(fc)/6–31G*//6–31G*	9·2	8·5
MP2(fc)/6–31G*//MP2(full)/6–31G*	11·7	11·4
MP2(full)/6–31G*//MP2(full)/6–31G*	11·8	11·5
MP3(fc)/6–31G*//MP2(full)/6–31G*	9·6	9·3
MP3(full)/6–31G*//MP2(full)/6–31G*	9·7	9·4
MP4(SDTQ,fc)/6–31G*//MP2(full)/6–31G*	9·7	9·4
MP4(SDTQ,full)/6–31G*//MP2(full)/6–31G*	9·8	9·5
MP2(fc)/6–31G**//MP2(full)/6–31G*	11·7	11·4
MP2(full)/6–31G**//MP2(full)/6–31G*	11·8	11·5
MP3(fc)/6–31G**//MP2(full)/6–31G*	9·5	9·2
MP3(full)/6–31G**//MP2(full)/6–31G*	9·6	9·3
MP4(SDTQ,fc)/6–31G**//MP2(full)/6–31G*	9·6	9·3
MP4(SDTQ,full)/6–31G**//MP2(full)/6–31G*	9·7	9·4
MP2(fc)/6–31 + G*//MP2(full)/6–31G*	11·8	11·5
MP3(fc)/6–31 + G*//MP2(full)/6–31G*	9·7	9·4
MP4(SDQ,fc)/6–31 + G*//MP2(full)/6–31G*	9·3	9·0
QCISD(fc)/6–31 + G*//MP2(full)/6–31G*	9·3	9·0
QCISD(T,fc)/6–31 + G*//MP2(full)/6–31G*	9·7	9·3
MP2(full)/6–311G**//MP2(full)/6–311G**	11·6	11·3
MP2(fc)/6–311G**//MP2(full)/6–311G**	11·4	11·1
MP3(fc)/6–311G**//MP2(full)/6–311G**	9·2	8·8
MP4(SDTQ,fc)/6–311G**//MP2(full)/6–311G**	9·4	9·1
MP4(SDQ,full)/6–31G*//MP4(SDQ,full)/6–31G*	9·3	9·0
MP4(SDTQ,full)/6–31G*//MP4(SDTQ,full)/6–31G*	9·8	9·5
Experiment (NMR)	8·4 ± 0·5[d]	

[a] From frequencies calculated at 6–31G*//6–31G* and scaled by 0·89 (for geometries at Hartree–Fock level).
[b] From fequencies calculated at MP2(full)/6–31G*//MP2(full)/6–31G* and scaled by 0·94 (for geometries at correlated levels).
[c] Ref. 23.
[d] Ref. 3b.

ched bonds or, in general, non-classical structures owing to an exaggeration of pair correlation effects (double excitations (D)). As soon as coupling between double excitations is included [at the MP3 level or the MP4(SDQ) level], the inversion barriers decrease to values close to experiment. Inclusion of triple (T) excitations at MP4 increases the barrier. This results from the known overestimation of triple contributions at this level of theory. In the same way, QCISD leads to values close to MP4(SDQ) while QCISD(T) increases the barrier values.[38,39]

Using the larger 6–311G** basis set leads to further improvement of calculated inversion barriers (Table 2) while diffuse functions or frozen core approximation have no influence on relative energies. Hence, the best description of **1** is achieved with a combination of the 6–311G** basis set, geometries optimized at the MP2 or MP4(SDQ) level, MP2 calculated ZPE effects, and a correlation method that handles T in a balanced way, e.g. CCSD(T).

Most semi-empirical methods fail completely to describe the $C_4H_5^+$ potential energy surface (PES) in the vicinity of **1**, but with a remarkable exception. Whereas MNDO, AM1 and PM3 find the planar structure **1a** as the only minimum, MINDO/3 correctly reproduces the curvature of the PES and finds a struc-

Table 3. Dissociation energy (*DE*) (kcal mol^{-1}) of **1b** into acetylene and the vinyl cation[a]

Computational level	*DE*	*DE* including ZPE[b,c]
6–31G*//6–31G*	90·8	82·5
MP2(full)/6–31G*//6–31G*	93·1	84·8
MP3(full)/6–31G*//6–31G*	93·7	85·4
MP4(SDTQ,full)/6–31G*//6–31G*	91·6	83·3
MP2(fc)/6–31G*//6–31G*	93·1	84·8
MP3(fc)/6–31G*//6–31G*	93·7	85·4
MP4(SDTQ,fc)/6–31G*//6–31G*	91·6	83·3
MP2(full)/6–31G*//MP2(full)/6–31G*	92·6	83·2
MP3(full)/6–31G*//MP2(full)/6–31G*	93·9	84·5
MP4(SDTQ,full)/6–31G*//MP2(full)/6–31G*	90·6	81·2
MP2(fc)/6–31G*//MP2(full)/6–31G*	92·4	83·0
MP3(fc)/6–31G*//MP2(full)/6–31G*	93·7	84·3
MP4(SDTQ,fc)/6–31G*//MP2(full)/6–31G*	90·4	91·0
MP2(full)/6–31G**//MP2(full)/6–31G*	92·2	82·8
MP3(full)/6–31G**//MP2(full)/6–31G*	93·9	84·5
MP4(SDTQ,full)/6–31G**//MP2(full)/6–31G*	90·7	81·3
MP2(fc)/6–31G**//MP2(full)/6–31G*	92·1	82·7
MP3(fc)/6–31G**//MP2(full)/6–31G*	93·7	84·3
MP4(SDTQ,fc)/6–31G**//MP2(full)/6–31G*	90·5	81·1
MP2(full)/6–311G**//MP2(full)/6–311G**	85·0	75·6
MP2(fc)/6–311G**//MP2(full)/6–311G**	84·6	75·2
MP3(fc)/6–311G**//MP2(full)/6–311G**	86·4	77·0
MP4(SDTQ,fc)/6–311G**//MP2(full)/6–311G**	83·2	73·8

[a] The energy of the non-classical (H-bridged) form was used. At the Hartree–Fock level the classical C_{2v} form is more stable by 7·0 kcal mol^{-1}. The bridged form is a transition state at the Hartree–Fock level but is the global minimum at all correlated levels.
[b] From frequencies calculated at 6–31G*//6–31G* and scaled by 0·89 (for geometries at Hartree–Fock level).
[c] From frequencies calculated at MP2(full)/6–31G*//MP2(full)/6–31G* and scaled by 0·94 (for geometries at correlated levels).

Table 4. Energy difference (kcal mol^{-1}) between the $^1A_1$ singlet state *E*(s) and $^3B_2$ triplet state *E*(t) of the cyclobutenyl cation

Computational level	*E*(s) – *E*(t)[a]	*E*(s) – *E*(t) including ZPE[a–c]
3–21G//3–21G	39·2	
6–31G*//3–21G	43·7	
6–31G*//6–31G*	41·3	37·6
MP2(fc)/6–31G*//6–31G*	70·7	74·4
MP3(fc)/6–31G*//6–31G*	64·0	60·3
MP4(SDTQ,fc)/6–31G*//6–31G*	67·4	63·7
MP2(full)/6–31G*//6–31G*	71·0	67·3
MP3(full)/6–31G*//6–31G*	64·2	60·5
MP4(SDTQ,full)/6–31G*//6–31G*	67·7	63·9
MP2(fc)/6–31G*//MP2(full)/6–31G*	71·7	67·9
MP3(fc)/6–31G*//MP2(full)/6–31G*	64·6	60·8
MP4(SDTQ,fc)/6–31G**//MP2(full)/6–31G*	68·1	64·3
MP2(full)/6–31G*//MP2(full)/6–31G*	71·8	68·0
MP3(full)/6–31G*//MP2(full)/6–31G*	64·7	60·9
MP4(SDTQ,full)/6–31G**//MP2(full)/6–31G*	68·3	64·5

[a] The spin projected energies are used for the triplet.
[b] Frequencies calculated at 6–31G* and scaled by 0·89 for 6–31G* geometries.
[c] Frequencies calculated at MP2(full)/6–31G* and scaled by 0·94 for geometries at correlated levels.

ture for **1b** which is similar to the higher level *ab initio* structures (1,3-bond length 1.74 Å, $\alpha = 149°$). Also, the ring inversion barrier of 9·8 kcal mol^{-1} compares with the *ab initio* results.

Since the experimentally determined ring inversion energy is a ΔG value, an entropy correction for the calculated barrier must be made. At the MP2(full)/6–31G* level[40] this increases the barrier by only 0·20 kcal mol^{-1} (150 K, 10^5 Pa).

The high stability of **1** with respect to dissociation into acetylene and vinyl cation has been established at various computational levels (Table 3). At the highest level [MP4(SDTQ,fc)/6–311G**//MP2(full)/6–311G** + ZPE], the homocyclopropenylium cation is stabilized against its dissociation products acetylene and the bridged vinyl cation by 73·8 kcal mol^{-1}. A major influence of electron correlation is not observed, as both sides of the dissociation equation benefit from non-classical delocalization.

We also examined the difference between singlet (**1b**) and triplet (**1c**) electronic states of the cation. When UHF/3–21G optimization on **1c** was started with a non-planar guess the geometry relaxed to a planar C_{2v} structure. The corresponding force constant matrix has only positive eigenvalues. The UHF/6–31G* and UMP2(full)/6–31G* structures (C_{2v} point group) are also minima on the potential energy surface. Of the four possible electronic states of the triplet (A_1, A_2, B_1, B_2), only three could be located. The $^3B_2$ state was the lowest in energy (and also had the least amount of spin contamination). The $^3A_1$ state was not located. At UHF/6–31G*, the relative energies are 0, 32·9 and 41·0 kcal mol^{-1} for the $^3B_2$, $^3B_1$ and $^3A_2$ state, respectively. Hence, only the $^3B_2$ state was refined further to correlated levels (Table 4). The computed absolute energies are compared with corresponding values of the singlet ground state $^1A_1$ (**1b**) and the energy differences are shown in Table 4. The triplet state clearly is higher in energy than the singlet.

Energetic evaluations

The homocyclopropenylium cation **1b** is related to two neutral hydrocarbons, bicyclo[1.1.0]butane **2** and cyclobutene, **4**. The energies of several homodesmotic and isodesmic bond separation reactions have been calculated (Table 5) in order to compare the strain energy of bicyclo[1.1.0]butane **2** with the comparably defined energy of the homocyclopropenylium cation **1b**. Such evaluations depend highly on the choice of the other species in the equations. Homodesmotic reactions are preferable since they balance errors in isodesmic treatments arising from different types of bonds.[41] Considering **1b** as a bicyclo[1.1.0]but-2-yl like structure and using the 2-propyl cation as a reaction product [equation (1a), Table 5], the homocyclopropenylium cation **1b** is more stable than bicyclobutane **2** [equation (1b), Table 5] by more than 18 kcal mol^{-1}. The 18·3 kcal mol^{-1} [from equations (1a) and (1b)] can be regarded a cation stabilization energy. The 18·3 kcal mol^{-1} derived from equations (1a) and (1b) also contain strain release due to partial opening of the central 1,3 bond on going from bicyclobutane **2** in equation (1b) to homocyclopropenylium cation **1b** in equation (1a). Using an artificial homocyclopropenylium cation geometry [MP2(full)/6–311G** optimized with C^1C^3 fixed at the bicyclobutane value, 1·506 Å; energy evaluated at MP4(SDTQ,fc)/6–311G**], an energy 13·9 kcal mol^{-1} higher than that for the fully optimized **1b** is obtained. Employing this value in the above procedure the cation stabilization energy is reduced to 4·4 kcal mol^{-1}. Treatment of **1b** as a cyclobutenyl like structure requires homodesmotic equations (1c) and (1d) (Table 5) and results in a 5·7 kcal mol^{-1} destabilization energy, corresponding to increasing strain on going from cyclobutene **4** in equation (1d) to homocyclopropenylium cation **1b** in equation (1c). Some isodesmic evaluations [equations (2)–(4), Table 5] are given for comparison. Equation (2) demonstrates the influence of the choice of reaction products in isodesmic equations. Both equations (2a) and (2b) are balanced for ring strain to a large degree. Equation (2a) is less endothermic than (2b) by nearly 30 kcal mol^{-1} owing to the higher stability of the 2-propyl cation compared with the cyclopropyl cation. An estimate of the relative strain energies of **1b** and **2**, as discussed above using equations (2a) and (2c), results in a value (30·3 kcal mol^{-1}) which is considerably higher than that derived from the homodesmotic equations (1a) and (1b). Reactions (3) and (4) are even less balanced for the different types of bonds involved and are roughly thermoneutral with respect to ring cleavage. No reasonable estimate for ring strain or cation stabilization energies can be made from the latter reactions.

No experimental heat of formation is known for **1b**, but is available[42] for an isomer, the methylcyclopropenyl cation. The energy of the homocyclopropenylium cation **1b** is 8·20 kcal mol^{-1} relative to the methylcyclopropenyl cation at MP4(SDTQ,fc)/6–311G**//MP2(full)/6–311G**. The experimental value of 237 kcal mol^{-1} for the methylcyclopropenyl cation leads to a heat of formation of about 245 kcal mol^{-1} for **1b**. The heat of formation of **1b**, estimated by several other methods, is presented in Table 6. Calibration is provided by the estimated ΔH_f for **2**. The atom equivalent method of Ibrahim and Schleyer[29] gives a value for **2** a few kcal mol^{-1} higher than experiment. Using the ZPE-corrected values from the bond separation reactions, good agreement with experiment[42] is achieved for **2** and **4**. Both the values for **1b** and **2** calculated with the atom equivalent approach are nearly the same as the homodesmotic bond separation values. Whereas at the Hartree–Fock level both posi-

Table 5. Bond separation reactions (kcal mol^{-1}) of the cyclobutenyl cation (**1b**), bicyclobutane (**2**) and cyclobutene (**4**)

	HF/6–31G*//6–31G*[a]		MP2(full)/6–31G*//MP2(full)/6–31G*[c]		MP4(SDTQ,fc)/6–311G**// MP2(full)/6–311G**[c]	
Homodesmotic reactions	E	Including ZPE[b]	E	Including ZPE[d]	E	Including ZPE[d]
(1a)[e] **1b** + 3 CH_3CH_3 → $CH_3CH_2CH_3$ + 2 $(CH_3)_2CHCH_2^+$ + $CH_3CH^+CH_3$ + 2 $CH_3CH_2^+$	−48·0	−42·4	−54·5	−48·8	−55·9	−50·2
(1b) **2** + 5 CH_3CH_3 → 2 $CH_3CH_2CH_3$ + 2 $CH_3CH(CH_3)_2$	−68·8	−61·8	−72·1	−66·1	−74·0	−68·0
(1c)[f] **1b** + CH_3CH_3 → $CH_3CH_2CH_2^+$ + $CH_3CH^+CH_3$ + allyl$^+$ + $CH_3CH{=}CH_2$ + 2 $CH_3CH_2^+$ + $CH_2{=}CH_2$	−46·1	−43·5	−42·9	−40·4	−44·2	−41·7
(1d) **4** + 3 CH_3CH_3 → 2 $CH_3CH_2CH_3$ + 2 $CH_3CH{=}CH_2$ + $CH_2{=}CH_2$	−33·0	−35·7	−33·0	−35·8	−33·3	−36·0
Isodesmic reactions						
(2a) **1b** + 2 CH_4 → cyclo-C_3H_6 + $CH_3CH^+CH_3$	−4·5	−1·0	−1·1	+2·5		
(2b) **1b** + 2 CH_4 → cyclo-$C_3H_5^+$ + $CH_3CH_2CH_3$	+23·2	+26·0	+29·9	+32·0		
(2c) **2** + 2 CH_4 → cyclo-C_3H_6 + $CH_3CH_2CH_3$	−37·9	−32·0	−33·5	−27·8		
(3) **1b** + 2 CH_4 → allyl$^+$ + $CH_3CH_2CH_3$	−15·1	−10·3	−6·7	−2·1		
(4) **1b** + 3 CH_4 → $CH_2{=}CH_2$ + CH_3CH_3 $CH_3CH^+CH_3$	−8·5	−5·4	−0·3	+2·3		

[a] The energies of the reference structures are taken from Refs 1f and 29 and the Erlangen Quantum Chemistry Archive.
[b] Energies are corrected for zero-point vibrational energy at HF/6–31G*.
[c] This work. The energies of some of the reference structures are taken from the Erlangen Quantum Chemistry Archive.
[d] Energies are corrected for zero-point vibrational energy at MP2(full)/6–31G*.
[e] Homodesmotic if **1b** is considered as 2-bicyclo[1.1.0]butyl cation.
[f] Homodesmotic if **1b** is considered as 3-cyclobutenyl cation.

Table 6. Heat of formation [ΔH_f (kcal mol^{-1})] estimates for **1b**, **2** and **4**

Species	Reaction[a]	ΔH_f HF/6–31G*//6–31G*	ΔH_f MP2(full)/6–31G*//MP2(full)/6–31G*	ΔH_f MP4(SDTQ,fc)/6–311G**//MP2(full)/6–311G**
1b	1a	235·4	241·8	243·2
2	1b	49·1	53·5	54·8
4	1d	43·1	43·2	43·4
1b	2a	241·5	238·0	—
1b	2b	241·0	235·0	—
2	2c	55·7	51·5	—
1b	3	246·3	238·2	—
1b	4	242·3	234·6	—

Species	Ibrahim and Schleyer[b]	MNDO	AM1	PM3	MINDO/3	Experiment[c]
1b	244·2	250·0	267·6	263·7	228·1	—
2	55·7	64·1	78·1	69·2	49·6	51·9
4	38·6	31·0	45·8	37·7	33·0	37·5

[a] The ZPE-corrected values from Table 5 have been used.
[b] Atom equivalent method.[29]
[c] Ref. 42.

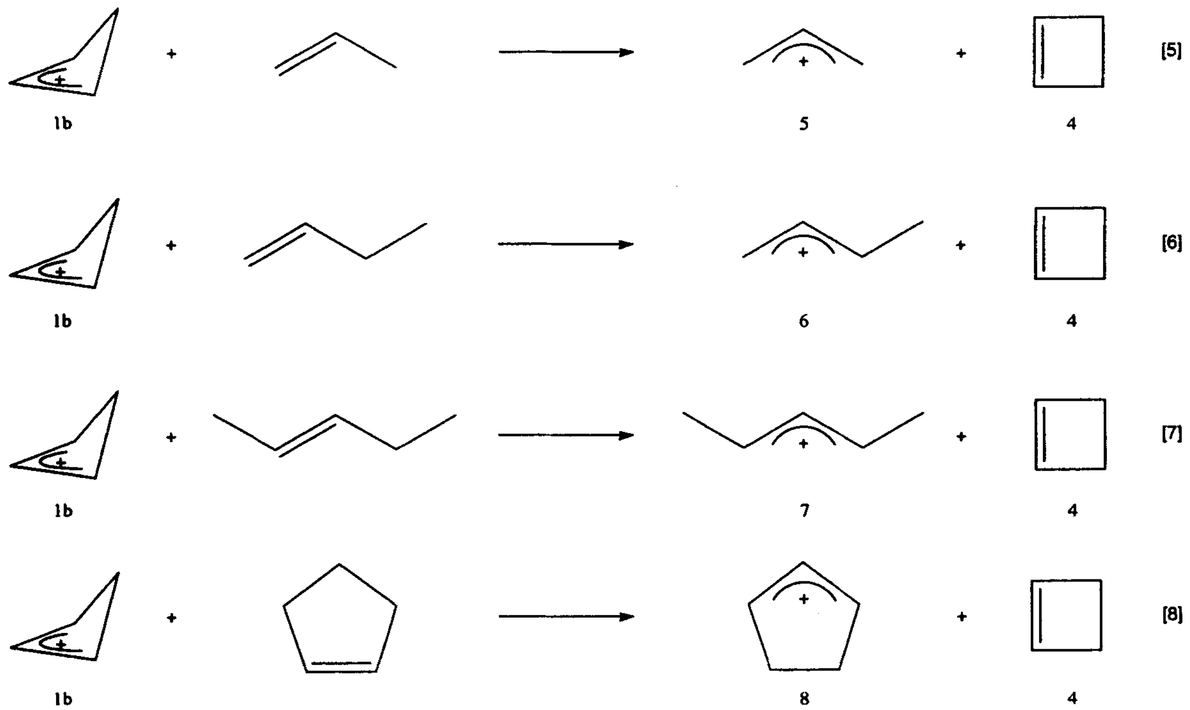

Scheme 1

tive and negative deviations are found, the MP2(full)/6–31G*//MP2(full)/6–31G* and MP4(SDTQ,fc)/6–311G**//MP2(full)/6–311G** calculations give more consistent results. Most of the values are in reasonable agreement with the atom equivalent heat of formation estimate. Taking into account the reliability of the atom equivalent approach and the experience from other strained systems, our best estimate of the heat of formation of **1** is about 244 kcal mol^{-1}.

It is noteworthy that all modern semi-empirical quantum chemical methods fail to reproduce the heat of formation of the homocyclopropenylium cation. The MINDO/3 energy is about 16 kcal mol^{-1} too low. MNDO, PM3 and AM1 compute energies which are 6–23 kcal mol^{-1} too high, and also give the wrong geometry. These methods find planar **1a** to be the only minimum. Nevertheless, if the results for **1** for all four of these methods are corrected for the errors for **2**, much better agreement is achieved.

Special attention has been paid to the relative energies of the homocyclopropenylium cation **1** and several allylic stabilized carbocations, using equations (5)–(8) (Scheme 1).

Whereas **1** is clearly more stable than the parent allyl cation **5** [by 17·2 kcal mol^{-1}, MP4(SDTQ,fc)/6–31G*//MP2(full)/6–31G*, equation (5), Table 7], additional stabilization of the allyl system by a terminal methyl group [1-methylallyl cation **6**, equation (6)] reduces this value to merely 3·0 kcal mol^{-1}. Another terminal methyl group in the allyl cation [equation (7)] reverses the order of stability. The 1,3-dimethylallyl cation **7** is favoured over **1** by 11·2 kcal mol^{-1}. Nearly

Table 7. Relative stabilities of the homocyclopropenylium cation and allylic systems (kcal mol^{-1})[a]

Equation	HF/6–31G*//(6–31G*	MP2(full)/6–31G*//MP2(full)/6–31G*	MP4(SDTQ,fc)/6–31G*//MP2(full)/6–31G*
5	+13·37	+18·96	+17·29
6	−0·88	+4·51	+2·81
7	−14·16	−10·27	−11·86
8	−14·33	−10·59	−12·27

[a] Energies are corrected for ZPE (HF/6–31G*, scaled by 0·89).

Table 8. Proton affinities and hydride ion affinities (kcal mol^{-1})[a]

Parameter	Species	HF/6–31G*//6–31G*	MP2(full)/6–31G* //MP2(full)/6–31G*	MP4(SDTQ,fc)/6–31G* //MP2(full)/6–31G*	Experiment
Proton affinity	Benzene/benzenonium cation	189·3	177·2	182·1	181·3
	Cyclooctatetraene/homotropylium cation	221·8	227·5	217·1[b]	
	Cyclopentadiene/cyclopent-1-en-3-yl cation	212·9	197·9	200·7	199·6
	trans-buta-1,3-diene/1-methylallyl cation	202·8	190·3	192·3	190·0
	Cyclobutadiene/homocyclopropenylium cation	243·6	231·8	230·2	
Hydride ion affinity	Benzenonium cation/cyclohexa-1,4-diene	240·42	251·71	252·84	
	Allyl cation/propene	279·32	296·45	321·22	
	1-Methylallyl cation/*trans*-but-2-ene	264·70	282·11	281·58	
	1,3-Dimethylallyl cation/*trans*-pent-2-ene	257·96	267·23	266·81	
	Cyclopent-1-en-3-yl cation/cyclopentene	266·80	266·90	266·39	
	Homocyclopropenylium cation/cyclobutene	264·69	277·48	278·65	
	Homocyclopropenylium cation/ *trans*-buta-1,3-diene	278·22	286·21	289·21	

[a] Energies are corrected for ZPE (HF/6–31G*, scaled by 0·89).
[b] MP4(SDQ,fc)//MP2(full)/6–31G*.

the same value ($11\cdot7$ kcal mol^{-1}) is obtained for the cyclic 'disubstituted' allyl cation, the cyclopent-1-en-3-yl cation **8** [equation (8)]. Only a small additional stabilization of $3\cdot0$ kcal mol^{-1} of the 'monosubstituted allyl cation' **1** can be found in accordance with the fact that orbital symmetry precludes effective stabilization by the bridging CH_2 group.

Whereas the HOMO can be stabilized by the bridging CH_2 group via interactions with the pseudo-π^* (CH_2) MO, a similar stabilization of the pseudo-π (CH_2) MO by the allyl LUMO is not possible because of symmetry (Scheme 2). In addition, two-electron stabilization of the allyl ion is reduced by four-electron destabilization between allyl HOMO and pseudo-π (CH_2) MO, thus preventing a higher stability of the homocyclopropenylium cation. These MO effects also lead to a reverse of the direction of the dipole moment as expected from comparison with unsaturated hydrocarbons (cf. computed charges in Figure 4). In cyclopropene, which has the same problem, the reverse of the dipole moment is verified experimentally.[43]

Other energetic consequences of aromatic stabilization are provided by proton affinities (*PA*, $C_nH_{m-1} + H^+ \rightarrow C_nH_m{}^+$) and hydride ion affinities (*HIA*, $C_nH_m{}^+ + H^- \rightarrow C_nH_{m+1}$), *PA* and *HIA* values for several systems are summarized in Table 8. Low values for the proton affinity are expected when highly stabilized (e.g. aromatic) systems such as benzene by protonation are converted into a less stabilized system. Thus the *PA* of benzene [$182\cdot1$ kcal mol^{-1} at MP4(SDTQ,fc)/6–31G*//MP2(full)/6–31G* + ZPE (HF/6–31G*)] can be taken as a lower limit for those of aromatic systems, where the cyclooctatetraene/homotropylium value ($217\cdot1$ kcal mol^{-1}) provides a comparison for the conversion of a formally antiaromatic species into its homoaromatic counterpart. The $PA = 230\cdot2$ kcal mol^{-1} for the antiaromatic cyclobutadiene (to give the homocyclopropenylium cation **1**) is even higher. The large destabilization of cyclobutadiene [cf. equation (9), MP2(full)/6–31G* + ZPE (HF/6–31G*)] as well as the stabilization of **1** contribute to this high *PA* value.

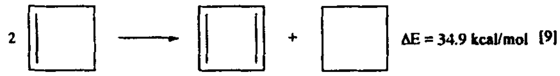

Smaller proton affinities are obtained for acyclic dienes or other cyclic dienes to give allylic cations with no additional (homoaromatic) stabilization (e.g. protonation of butadiene to give the methylallyl cation **6**, $192\cdot3$ kcal mol^{-1}, or protonation of cyclopentadiene to give cyclopent-1-en-3-yl cation **8**, $200\cdot7$ kcal mol^{-1}; cf. Table 8).

The results are similar for hydride ion affinities. (Note that the absolute values of the calculated HIAs are not very reliable. The 6–31G* basis set, which is well suited for carbocations and hydrocarbons, is much too small for anions. Especially the lack of diffuse functions leads to unreliable geometries and energies. Since here only the hydride ion is concerned, relative energies are still reasonable.) The homocyclopropenylium ion *HIA*s ($278\cdot7$ kcal mol^{-1}, to give cyclobutene; $289\cdot2$ kcal mol^{-1}, to give butadiene) are comparable in energy to the monosubstituted methylallyl cation ($281\cdot6$ kcal mol^{-1}). The more highly stabilized 1,3-dimethylallyl cation has a lower *HIA* ($266\cdot8$ kcal mol^{-1}) and the parent allyl cation a much higher *HIA* ($321\cdot2$ kcal mol^{-1}). Hence the homocyclopropenylium ion reveals similar behaviour to a monosubstituted allyl cation with only small additional (homo)aromatic stabilization.

NMR chemical shifts

^{13}C NMR chemical shifts of saturated hydrocarbons and aliphatic carbocations can, in general, be estimated satisfactorily[14,44,45] using the IGLO procedure of Kutzelnigg and Schindler.[32] The performance for

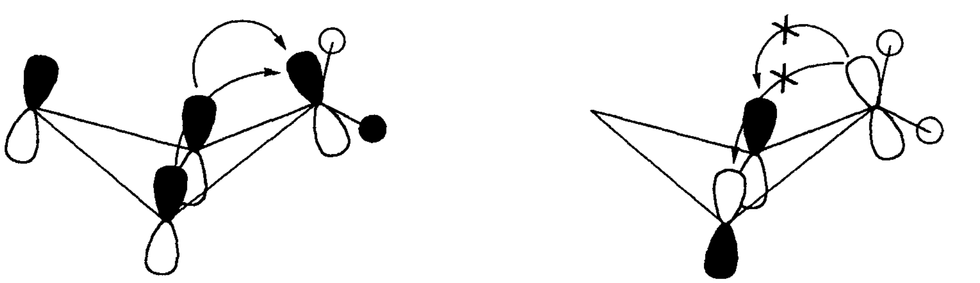

HOMO (allyl) - pseudo-π* (CH_2) interaction LUMO (allyl) - pseudo-π (CH_2) interaction

Scheme 2

unsaturated systems is less satisfactory.[33,34] The computed ^{13}C NMR chemical shifts of carbocations in particular are very sensitive to small changes in geometry and very accurate structures as obtained from high-level quantum chemical calculations are often a prerequisite to achieve good agreement between experimental and computed ^{13}C NMR data.[46] Since gegenion and solvent effects play a minor role in carbocation ^{13}C NMR spectroscopy,[47] calculations on isolated species give a reasonable model in most cases.[46]

We have applied the IGLO method to the HF/6–31G*, MP2(full)/6–31G*, MP2(full)/6–311G** and MP4(SDQ)/6–31G* geometries of **1** (see Figure 1), using the IGLO basis sets DZ (double zeta) and II (triple zeta plus polarization functions for C and H) in addition to the standard 6–31G* basis set. The data are summarized in Table 9.

In 1975 Olah and co-workers' NMR experiments showed that at temperatures below −100 °C a puckered (non-planar) homocyclopropenylium cation could be 'frozen out'.[3] During cooling from −60 to −100 °C line broadening and splitting of the δ^1H (CH_2) signal indicated the non-equivalence of the methylene protons as a consequence of the puckered structure of **1**.

Calculated chemical shifts of **1b** verify the non-equivalence of the CH_2 protons suggesting a shift difference of 0·9 ppm, which compares well with the experimental value of 0·8 ppm.[3] However, contrary to experiment, the $\delta H_{exo} - \delta H_{endo}$ difference is found to be negative at all levels of theory, thus confirming Schindler's earlier results.[14] The assignments of ^1H signals in the experimental spectrum may have been reversed. Apart from this, the $\delta H_{exo} - \delta H_{endo}$ shift difference shows only a small dependence on the puckering angle α or the 1,3-distance over the range investigated (see below). Contrary to the homotropylium cation (**3**), the 1,3-distance in **1** seems not to be a sensitive indicator of those changes in the electronic structure when going from the puckered C_s to the planar C_{2v} structure. Likewise, the magnetic susceptibility χ only changes by 3 units on going from C-1 C-3 = 1·4 to 1·9 Å. Obviously, both $\Delta\delta H$ and $\Delta\chi$ are related to the ring size of **1** and the large value of the puckering angle (144·5°) as compared with that of **3** (111·7°).[11]

The computed ^{13}C chemical shifts of **1b**, using the geometry optimized at the HF/6–31G* level, deviate by 3–26 ppm from the experimental values.[3b] While deviations of 3 and 7 ppm (for C-2 and CH_2) are fairly good for geometries at the Hartree–Fock level, the difference of 26 ppm (for C-1) is unacceptably large. Use of the MP2(full)/6–31G* structure improves the IGLO value by more than 19 ppm for the C-1 position, but for C-2 the divergence increases to 16 ppm. The MP2(full)/6–311G** geometry results only slight additional improvement over the DZ//MP2(full)/6–31G* values. Both geometries are nearly the same. Even IGLO basis II, which often performs better on strained molecules,[48] gives nearly the same chemical shifts (Table 9); only the C-2 value improves (by *ca* 4 ppm), but is still 16 ppm from the experimental value.

In general, deviations up to 5 ppm are considered to be within both experimental and IGLO error. This value is still exceeded here at the best level ($\Delta\delta$ ^{13}C = 9 and 16 ppm for C-1 and C-2, respectively). Chemical shifts calculated for the Hartree–Fock and MP2 geometries differ considerably. This indicates that the chemical shifts highly depend on the geometry of the

Table 9. Comparison of calculated and experimental ^{13}C chemical shifts (ppm vs TMS)

	1a (C_{2v})			**1b** (C_s)		
Method	CH_2	C-1	C-2	CH_2	C-1	C-2
IGLO/DZ//6–31G*[a]	35·31	162·56	257·11	47·05	159·71	190·30
IGLO/DZ//MP2(full)/6–31G*[a]	36·74	167·00	261·09	49·72	140·85	206·85
IGLO/II//MP2(full)/6–31G*[b]	36·34	160·28	258·75	44·67	134·84	197·11
IGLO/DZ//MP2(full)/6–311G**[a]	37·28	168·21	262·26	50·41	142·74	207·56
IGLO/II//MP2(full)/6–311G**[b]	36·81	161·48	259·93	45·47	136·74	197·91
GIAO-SCF/TZP/DZP//MP2(full)/6–31G*[c]				48·1	136·4	198·6
GIAO-MP2/TZP/DZP//MP2(full)/6–31G*[c]				55·6	127·7	191·0
GIAO-SCF/TZP/DZP//MP2(full)/6–311G**[c]				49·53	140·36	201·76
GIAO-MP2/TZP/DZP//MP2(full)/6–311G**[c]				55·88	128·67	191·41
IGLO/6–31G*//MP4(SDQ)/6–31G*				44·6	134·9	190·5
GIAO-SCF/TZP/DZP//MP4(SDQ)/6–31G*[c]				48·9	141·1	195·6
GIAO-MP2/TZP/DZP//MP4(SDQ)/6–31G*[c]				56·4	131·1	189·3
Experiment[d]				54·0	133·5	187·6

[a] IGLO/DZ values are vs CH_4 (correction for TMS is *ca* 0).
[b] IGLO/II values are corrected for TMS by −5·7 ppm.
[c] TZP/DZP: polarized (α = 0·8) triple zeta basis for carbon (51111/311/1), polarized (α = 0·8) double zeta basis for hydrogen (31/1); cf. Ref. 37.
[d] Ref. 3b.

four-membered ring. We first investigated the dependence of the ^{13}C chemical shifts on critical geometry parameters[11,44c,49] [geometries are optimized at the MP2(full)/6–31G* level with fixed 'critical parameters.' Small changes in such 'critical parameters' result in large variations of chemical shifts]. Here we investigated the dependence of the homocyclopropenylium cation ^{13}C chemical shifts on the half opened central C-1—C-3 bond length (Figure 2). For a wide range of structures round the structure of the fully optimized minimum the influence on the chemical shift of the CH_2 carbon is small, large variations are found for C-1 and C-2. The trends for the chemical shifts of C-1 and C-2 on the alteration of *d*(C-1—C-3) lead into opposite directions. Nevertheless, average errors of the shifts calculated for the partially optimized structures indicate the C-1—C-3 bond length to be slightly longer.

A new method (GIAO-MP2) which has been developed very recently[34] allows the calculation of chemical shifts at correlated levels using the GIAO approach[50] to ensure gauge invariance. We have applied this method to the MP2(full)/6–31G*, MP2(full)/6–311G** and MP4(SDQ,fc)/6–31G* geometries of the homocyclopropenylium cation (cf. Table 9). While the chemical shifts computed at the Hartree–Fock level are similar to the IGLO values, the correlated MP2 level greatly improves the agreement of the chemical shifts with the experimental data.[3] At the GIAO-SCF level the average

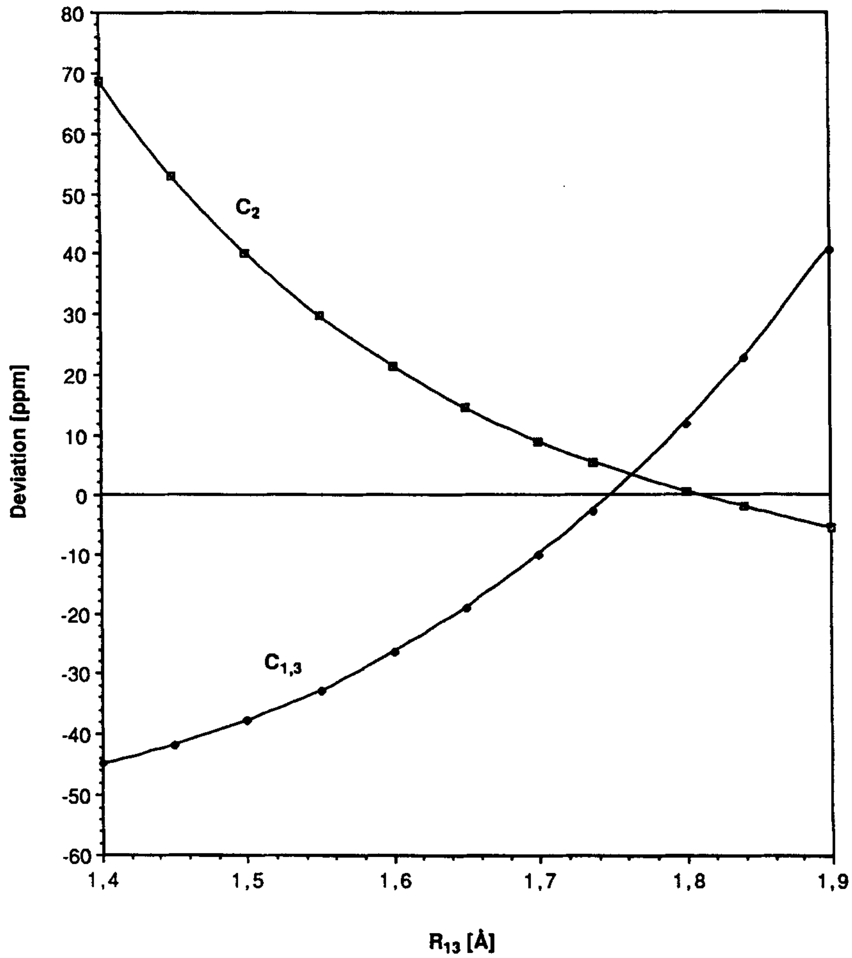

Figure 2. Differences between experimental and computed ^{13}C chemical shifts of the homocyclopropenylium cation as a function of the bond length C-1—C-3. Geometries are optimized at the MP2(full)/6–31G* level with fixed C-1—C-3 bond length. Chemical shifts are computed using the 6–31G** standard basis set

error of 8·5 ppm is similar to the IGLO/II average error (7·4 ppm). At the correlated GIAO-MP2 level this average error decreases significantly to 3·5 ppm [MP2(full)/6–311G** geometry) and to 1·9 ppm (MP4(SDQ)/6–31G* geometry]. These results are in the range of computational and experimental error.

Homoaromaticity

Following Winstein, the requirements for homoaromaticity can be summarized:[5–7]

(a) the system in question should possess a 1,3-bond, closing the cyclic conjugation;
(b) the 1,3 bond order should be significantly greater than zero;
(c) the orbital overlap of the participating p-AOs at the centres involved should be between pure σ and pure π in character; and
(d) the $(4n + 2)\pi$-electrons are delocalized significantly over the closed cycle which results.

The problem can be considered in the following way using structures **A**, **B** and **C** as models.

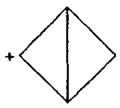
A

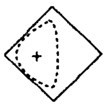
B

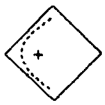
C

Structure **A** has a C-1—C-3 bond comparable to the CC bonds of cyclopropane or the central CC bond of bicyclobutane. Structure **C** is a 'classical' cyclopolyenyl cation with weak through-space interactions between centres 1 and 3. Form **B** represents a homoaromatic structure characterized by stronger through-space 1,3-interactions. These may or may not lead to 1,3-bonding in the sense of Winstein's postulate.

Depending on the energetic relationship between **A**, **B** and **C**, one can distinguish among four situations:

(1) there is a single minimum on the PES which corresponds to one of the classical structures **A** or **C**; homoaromaticity is not relevant;
(2) the single minimum on the PES corresponds to the homoaromatic **B**; structure **B** should be distinguished clearly from the classical structures **A** and **C** by unusual electronic and geometrical features;
(3) there are two minima on the PES corresponding to the two classical structures **A** and **C**; if so, only the transition state between these two minima (e.g. **B**) should possess homoaromatic character;
(4) if there are three minima on the PES corresponding to **A**, **B** and **C**, structure **B** should be the most stable unless other electronic factors overrule homoaromatic stabilization.

The following points are pertinent.

(a) the 1,3-distance of **1b**, 1·75 Å [MP4(SDQ)/6–31G*], is clearly intermediate between the C-1—C-3 bond length of the three-membered ring in bicyclobutane (1·47 Å) and the 1·98 Å 1,3-separation in the planar form **1a**;
(b) the stabilization of **1b**, between 3 (compared with the methylallyl cation) and 8·4 kcal mol^{-1} (the barrier to planarity, including strain release), is comparable to the estimated homoaromatic stabilization of the homotropylium cation (4 kcal mol^{-1});[11]
(c) the differences in ^{13}C NMR chemical shifts between C-1(C-3) and C-2 become less as the flap angle is decreased from 180° or increased from the bicyclobutane value (122·3°, Figure 2);
(d) likewise, in **1b** the positive charge is almost uniformly delocalized over the homoaromatic three-membered ring (cf. Figure 4).

Similar 1,3-bond length and charge distribution effects have been found in the homotropylium cation **3**.[11] In addition, the CC bonds in the homoaromatic seven-membered ring of **3** all have nearly the same length (1·400 ± 0·005 Å).[11] The calculated bond orders (Figure 3), ca. 1·5, also are typical for delocalized 6π electron systems. For **1b**, the C-1—C-2 bond length (1·387 Å) is longer than that in the cyclopropenyl cation (1·363–1·379 Å obtained for various substituted ions) [from structures at various correlated levels (geometries taken from the Erlangen Quantum Chemistry Archive)], but again the calculated bond orders, 1·35 and 0·38 for C-1—C-2 and C-1—C-3, respectively (Figure 4), are close to the ideal value (one third of a π-bond arising from the two π-electrons in the three-membered ring). The planar form **1a** shows similar features as the allyl cation. C-1—C-3 bond orders for allyl cation (0·21) and planar homocyclopropenylium cation (0·24, Figure 5) are nearly the same, and are much smaller than that in **1b**. No additional electronic interaction, except for steric reasons (the 1,3-distance in **1a** is *ca* 0·2 Å shorter than in the allyl cation), can be found in **1a**, compared with the allyl cation.

Cremer and Kraka[5a,51] gave two conditions for the existence of a covalent bond between two atoms A and B, namely (1) that A and B are connected by a path of maximum electron density (necessary condition) and (2) that the local energy density is negative (stabilizing) at the bond critical point[51b,52] (sufficient condition). Applying these criteria to the calculated MP2(full)/6–31G* response density[9] of both the homotropylium cation **3** and ion **1b** reveals that neither C-1–C-7 nor C-1–C-3 are connected by a path of maximum electron density. On this basis, the homoaromatic bond as

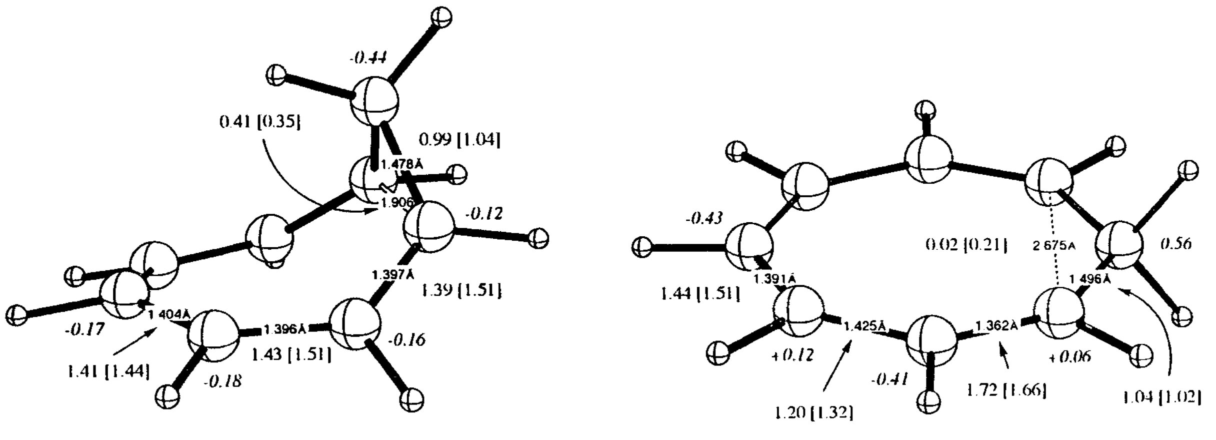

C_s C_{2v}

Figure 3. MP2 total response electron densities (given in square brackets), NPA bond orders (Wiberg bond index) and NPA charges for the homotropylium ion at MP2(full)/6–31G*//MP2(full)/6–31G*

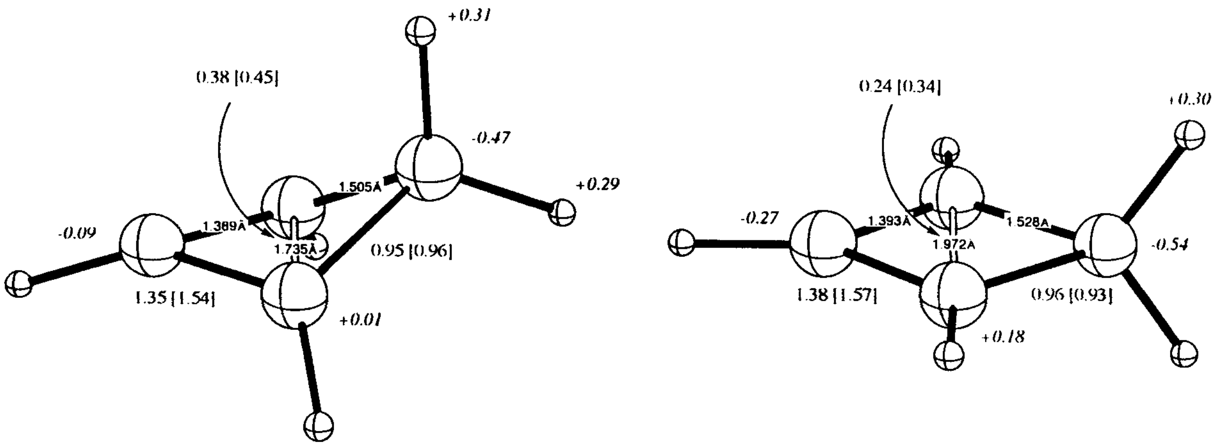

C_s C_{2v}

Figure 4. MP2 total response electron densities [for MP4(SDQ)/6–31G* geometries given in square brackets], NPA bond orders (Wiberg bond index) and NPA charges for the homocyclopropenylium ion at MP2(full)/6–31G*//MP2(full)/6–31G*

required by Winstein does not exist. However, the build-up of electron density in the internuclear region of both **1b** and **3** is significantly larger than that observed for planar **3** or ion **1a**. Using these density values to calculate an interaction index similar to the bond orders for conventional bonds, one obtains 0·45 for **1b** and 0·35 for **3** [MP2(full)/6–31G* response densities]. These compare well with Wiberg bond indices of 0·38 and 0·41 (see Figures 4 and 3). This density built up results from overlapping p-orbitals, shown in Figures 5 and 6 as contour plots of the bonding NLMOs (natural localized molecular orbital)[8] in a plane perpendicular to the ring plane of **1b** and to the C-1–C-2–C-6–C-7 plane of **3**. In both cases, the overlap between the p-orbitals is between σ and π as suggested by Winstein.

Similar interaction indices, bond orders and characteristics of the bonding NLMO are found not only for **1b** and **3** but also for the isoelectronic homodiboriranide[10] (Figures 7 and 8). In contrast to the usual description with formal charges, the boron atoms

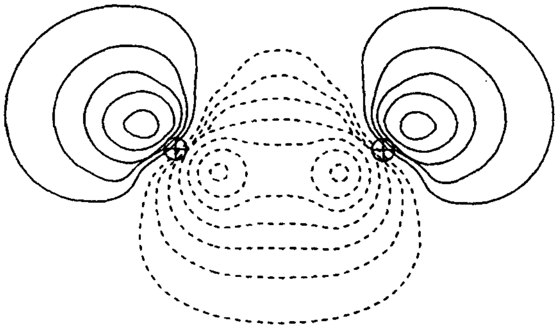

Figure 5. Contour plot of the 1,3-bonding orbital (NLMO) for the homotropylium ion at MP2(full)/6–31G*//MP2(full)/6–31G* in a plane perpendicular to the $C^1C^2C^6C^7$ plane

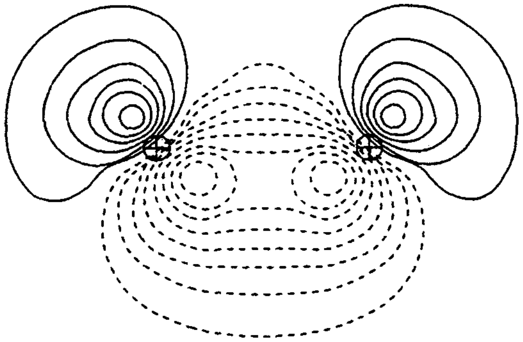

Figure 6. Contour plot of the 1,3-bonding orbital (NLMO) for the homocyclopropenylium ion at MP2(full)/6–31G*//MP2(full)/6–31G* in a plane perpendicular to the $C^1C^2C^3$ plane

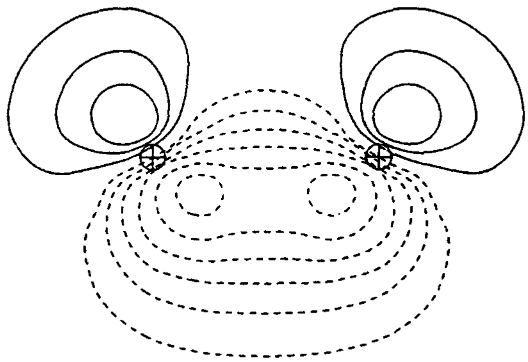

Figure 8. Contour plot of the 1,3-bonding orbital (NLMO) for the homodiboriranide ion at HF/6–31G*//MP2(full)/6–31G* in a plane perpendicular to the $B^1C^2B^3$ plane

in the homodiboriranide anion are positively charged (+0·35 in the NPA). Hence fewer electrons are available for the 1,3-BB overlap than in **1b**. This results in a lower bond order (0·23) and a slightly longer 1,3-bond length (1·859 Å).

We conclude that homoaromatic character is a result of strong through-space interactions caused by p–p overlap between the interacting centres. Its consequences are delocalization of $(4n+2)\pi$-electrons accompanied by an equalization of atomic charges, bond lengths and ^{13}C chemical shifts. Clearly, **1b** is a prototype for homoaromatic character.

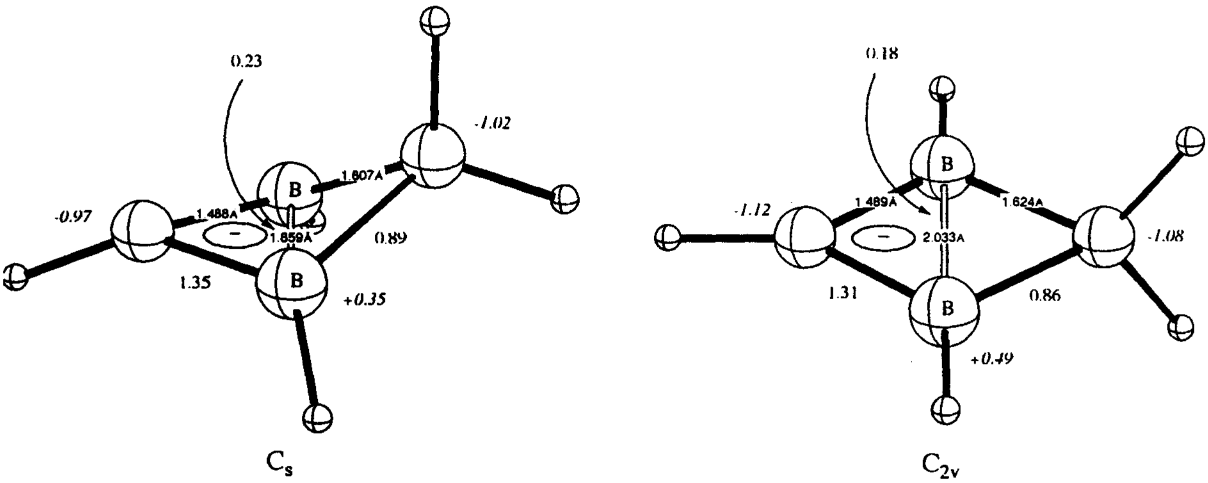

Figure 7. NPA bond orders (Wiberg bond index) and NPA charges for the homodiboriranide ion at HF/6–31G*//MP2(full)/6–31G*

ACKNOWLEDGEMENTS

Calculations were carried out at the Rechenzentrum Berlin Mitte (IBM 4381), at Erlangen (Convex C220). with the Cray XMP/416 of the NSC at Linköping, Sweden, and with the Cray YMPs of the LRZ München and the HLRZ Jülich. The work in Erlangen was supported by the Deutsche Forschungsgemeinschaft and Convex Computer Corporation and at Karlsruhe by the Fonds der Chemischen Industrie. Work at Göteborg was supported by the Swedish Natural Science Research Council (NFR) and the Nationellt Superdatorcentrum (NSC), Linköping. A. H. Otto is especially grateful to Dr Schiller and Mr Gasinsky for their kind assistance with many of the calculations. We thank M. Bühl for the QCISD(T) calculations.

REFERENCES

1. (a) Ch. Roberts and J. C. Walter, *J. Chem. Soc., Perkin Trans. 2* 879 (1983), (b) A. H. Goldberg and D. A. Dougherty, *J. Am. Chem. Soc.* **105**, 284 (1983); (c) J. Pacansky and M. Yoshimine, *J. Phys. Chem.* **89**, 1880 (1985); (d) R. L. Disch, J. L. Schulman and M. L. Sabio, *J. Am. Chem. Soc.* **107**, 1904 (1985); (e) W. J. Hehre, L. Radom, P. v. R. Schleyer and J. A. Pople. *Ab Initio Molecular Orbital Theory*. Wiley, New York (1986); (f) D. Cremer and E. Kraka, *Mol. Struct. Energ.* **7** (Struct. React.), 65–138 (1988), and references cited therein; (g) K. B. Wiberg, *Angew. Chem., Int. Ed. Engl.* **25**, 312 (1986); (h) R. Jain, M. B. Sponsler, F. D. Comes and D. A. Dougherty, *J. Am. Chem. Soc.* **110**, 1356 (1988); (i) D. A. Dougherty, *J. Phys. Org. Chem.* **2**, 161 (1988); (j) P. B. Shevlin and M. L. McKee, *J. Am. Chem. Soc.* **111**, 519 (1989); (k) H. Fujimoto, T. Yabuki and K. Fukui, *J. Mol. Struct.* **198**, 267 (1989); (l) F. Gerson, X.-Z. Qin, C. Ess and E. Kloster-Jensen, *J. Am. Chem. Soc.* **111**, 6456 (1989); (m) D. B. Kitcher, J. A. Jackson and L. C. Allen, *J. Am. Chem. Soc.* **112**, 3408 (1990); (n) K. B. Wiberg, S. T. Waddel and R. E. Rosenberg, *J. Am. Chem. Soc.* **112**, 2184 (1990); (o) J. D. Evanseck, J. Mareda and K. N. Houk, *J. Am. Chem. Soc.* **112**, 73 (1990); (p) E. W. Della and D. K. Taylor, *Aust. J. Chem.* **43**, 945 (1990); (q) S. Olivella and A. Sole, *J. Am. Chem. Soc.* **113**, 87 (1991); (r) P. K. Chou and S. R. Kass, *J. Am. Chem. Soc.* **113**, 697 (1991); (s) K. B. Wiberg, C. M. Hadad, S. Sieber and P. v. R. Schleyer, *J. Am. Chem. Soc.* **114**, 5820 (1992).
2. (a) Refs 1s, 11, 44, 45, 46a,b; (b) M. Bremer, P. v. R. Schleyer. K. Schötz, M. Kausch and M. Schindler. *Angew. Chem.* **99**, 795 (1987); *Angew. Chem., Int. Ed. Engl.* **26**, 761 (1987); (c) P. v. R. Schleyer, T. W. Bentley, W. Koch, A. J. Kos and H. Schwarz, *J. Am. Chem. Soc.* **109**, 6953 (1987); (d) M. Saunders, K. E. Laidig, K. B. Wiberg and P. v. R. Schleyer, *J. Am. Chem. Soc.* **110**, 7652 (1988), and references cited therein; (e) P. v. R. Schleyer and M. Bremer, *J. Org. Chem.* **53**, 2362 (1988); (f) P. Buzek, P. v. R. Schleyer and S. Sieber, *Chemie Unserer Zeit* **26**, 116 (1992), and references cited therein; (g) P. v. R. Schleyer and J. W. de M. Carneiro, *J. Comput. Chem.* **13**, 997 (1992).
3. G. A. Olah, J. S. Staral and G. Liang, *J. Am. Chem. Soc.* **96**, 6233 (1974); (b) G. A. Olah, J. S. Staral, R. J. Spear and G. Liang, *J. Am. Chem. Soc.* **97**, 5489 (1975).
4. C. Krüger, P. J. Roberts, Y.-H. Tsay and J. B. Koster, *J. Organomet. Chem.* **78**, 69 (1974).
5. For reviews on homoaromaticity, see (a) E. Kraka and D. Cremer, in *Theoretical Models of Chemical Bonding. The Concept of the Chemical Bond*, edited by Z. B. Maksic, Vol. 2, p. 453. Springer, Heidelberg (1990); (b) P. M. Warner, in *Topics in Nonbenzenoid Aromatic Character*, edited by T. Nozoe, R. Breslow, K. Hafner, S. Ito and I. Murata, Vol. 2. Hirokawa, Tokyo (1979); (c) L. A. Paquette, *Angew. Chem., Int. Ed. Engl.* **17**, 106 (1978); (d) R. F. Childs, *Acc. Chem. Res.* **17**, 347 (1984); (e) D. Cremer, E. Kraka, T. S. Slee R. F. W. Bader, C. D. H. Lau, T. T. Nguyen-Dang and P. J. MacDougall, *J. Am. Chem. Soc.* **105**, 5069 (1983).
6. S. Winstein, *J. Am. Chem. Soc.* **81**, 6524 (1959).
7. (a) S. Winstein, *Q. Rev. Chem. Soc.* **23**, 141 (1969); (b) S. Winstein, in *Carbonium Ions*, edited by G. A. Olah and P. v. R. Schleyer, Vol 3, pp. 965–1005. Wiley, New York (1972).
8. (a) A. E. Reed, R. B. Weinstock and F. Weinhold, *J. Chem. Phys.* **83**, 735 (1985); (b) A. E. Reed, L. A. Curtis and F. Weinhold, *Chem. Rev.* **88**, 899 (1988).
9. E. Kraka, J. Gauss and D. Cremer, *J. Mol. Struct. (Theochem)* **234**, 95 (1991).
10. P. Willershausen, C. Kybart, N. Stamatis, W. Massa, M. Bühl, P. v. R. Schleyer and A. Berndt, *Angew. Chem.* **104**, 1278 (1992).
11. D. Cremer, F. Reichel and E. Kraka, *J. Am. Chem. Soc.* **113**, 9459 (1991); (b) Ref. 2f.
12. R. C. Haddon, *J. Am. Chem. Soc.* **97**, 3608 (1975).
13. A. J. P. Devaquet and W. J. Hehre, *J. Am. Chem. Soc.* **96**, 3644 (1974).
14. M. Schindler, *J. Am. Chem. Soc.* **109**, 1020 (1987).
15. D. R. Kelsey, *J. Chem. Res. (S)* 44 (1986).
16. (a) W. L. Jorgensen, *J. Am. Chem. Soc.* **98**, 6784 (1976); (b) R. C. Haddon, *J. Org. Chem.* **44**, 3608 (1979).
17. (a) P. C. Hariharan and J. A. Pople, *Chem. Phys. Lett.* **16**, 217 (1972); (b) P. C. Hariharan and J. A. Pople, *Theor. Chim. Acta* **28**, 213 (1973).
18. J. M. Bofill, J. Castells, S. Olivella and A. Sole, *J. Org. Chem.* **53**, 5148 (1988).
19. M. J. S. Dewar and W. Thiel, *J. Am. Chem. Soc.* **99**, 4899, 4907 (1977).
20. M. J. S. Dewar, E. G. Zoebisch, E. F. Healy and J. J. P. Stewart, *J. Am. Chem. Soc.* **107**, 3902 (1985).
21. J. J. P. Stewart, *J. Comput. Chem.* **10**, 221 (1989).
22. R. C. Bingham, M. J. S. Dewar and D. H. Lo, *J. Am. Chem. Soc.* **97**, 1285, 1294, 1302, 1307 (1975).
23. R. C. Haddon and K. Raghavachari, *J. Am. Chem. Soc.* **105**, 118 (1983).
24. J. S. Binkley, R. A. Whiteside, R. Krishnan, R. Seeger, D. J. DeFrees, H. B. Schlegel, S. Topiol, L. R. Kahn and J. A. Pople, *Gaussian 80*. Carnegie-Mellon Quantum Chemistry Publishing Unit Pittsburgh, PA; M. J. Frisch, M. Head-Gordon, G. W. Trucks, J. B. Foresman, H. B. Schlegel, K. Raghavachari, M. A. Robb, J. S. Binkley, C. Gonzalez, D. J. Defrees, D. J. Fox, R. A. Whiteside, R. Seeger, C. F. Melius, J. Baker, R. Martin, L. R. Kahn, J. J. P. Stewart, S. Topiol and J. A. Pople, *Gaussian 90*. Gaussian, Pittsburgh, PA (1990).

25. R. D. Amos and J. E. Rice, *CADPAC 4.1: CADPAC: The Cambridge Analytic Derivatives Package*, Issue 4.1. Cambridge, UK (1989).
26. J. Gauss and D. Cremer, *Adv. Quantum Chem.* **23**, 205 (1992), and references cited therein.
27. (a) C. Møller and M. Plesset, *Phys. Rev.* **46**, 618 (1934); (b) J. A. Pople, J. S. Binkley and R. Seeger, *Int. J. Quantum Chem. Symp.* **10**, 1 (1976).
28. (a) Ref. 1e, p. 34; (b) J. A. Pople, M. Head-Gordon and K. Raghavachari, *J. Chem Phys.* **87**, 5968 (1987).
29. M. R. Ibrahim and P. v. R. Schleyer, *J. Comput. Chem.* **6**, 157 (1985).
30. G. Rauhut, J. Chandrashekar and T. Clark, unpublished work (1991).
31. J. Baker, *J. Comput. Chem.* **8**, 563 (1987).
32. (a) W. Kutzelnigg, *Isr. J. Chem.* **19**, 193 (1989); (b) M. Schindler and W. Kutzelnigg, *J. Chem. Phys.* **76**, 1919 (1982).
33. W. Kutzelnigg, M. Schindler and U. Fleischer, in *NMR, Basic Principles and Progress*, (eds P. Diehl, E. Fluck and R. Kosfeld) p. 165. Springer, Berlin, (1990).
34. J. Gauss, *Chem. Phys. Lett.* **191**, 614 (1992).
35. J. F. Stanton, J. Gauss, J. D. Watts, W. J. Lauderdale, R. J. Bartlett, *ACES II, an Ab Initio Program System*. University of Florida, Gainesville, FL (1991, 1992).
36. J. F. Stanton, J. Gauss, J. D. Watts, W. J. Lauderdale, R. J. Bartlett, *Int. J. Quant. Chem. Symp.* **26**, 879 (1992).
37. A. Schäfer, H. Horn and R. Ahlrichs, *J. Chem. Phys.* **97**, 2571 (1992).
38. Z. He and and D. Cremer, *Int. J. Quant. Chem. Symp.* **25**, 43 (1991).
39. J. E. Del Bene, D. H. Aue and I. Shavitt, *J. Am. Chem. Soc.* **114**, 1631 (1992).
40. W. J. Hehre, L. Radom, P. v. R. Schleyer and J. A. Pople, *Ab Initio Molecular Orbital Theory*, p. 251, Wiley, New York (1986).
41. P. George, M. Trachtman, C. W. Bock and A. M. Brett, *Tetrahedron* **32**, 317 (1976).
42. (a) S. G. Lias, J. E. Bartmess, J. F. Liebmann, J. L. Holmes, R. D. Levin and W. G. Mallard, *J. Phys. Chem. Ref. Data* **17** Suppl. 1 (1988); (b) F. P. Lossing and J. L. Holmes, *J. Am. Chem. Soc.* **106**, 6917 (1984).
43. W. J. Hehre, L. Radom, P. v. R. Schleyer and J. A. Pople, *Ab Initio Molecular Orbital Theory*, p. 330. Wiley, New York (1986).
44. (a) J. W. Carneiro, P. v. R. Schleyer, W. Koch and K. Raghavachari. *J. Am. Chem. Soc.* **112**, 4066 (1990); (b) P. v. R. Schleyer, W. Koch, B. Liu and U. Fleischer, *J. Chem. Soc., Chem. Commun.* **16**, 1098 (1989); (c) P. v. R. Schleyer, J. W. Carneiro, W. Koch and K. Raghavachari, *J. Am. Chem. Soc.* **111**, 5475 (1989); (d) M. Schindler and W. Kutzelnigg, *J. Chem. Phys.* **76**, 1919 (1982); (e) P. v. R. Schleyer, K. Laidig, K. B. Wiberg, M. Saunders and M. Schindler, *J. Am. Chem. Soc.* **110**, 300 (1988); (f) M. Saunders, K. E. Laidig, K. B. Wiberg and P. v. R. Schleyer, *J. Am. Chem. Soc.* **110**, 7652 (1988); (g) P. Buzek, P. v. R. Schleyer, S. Sieber, W. Koch, J. W. Carneiro, H. Vančik and D. E. Sunko, *J. Chem. Soc., Chem. Commun.* **18**, 671 (1991); (h) M. Bremer, K. Schötz, P. v. R. Schleyer, U. Fleischer, M. Schindler, W. Kutzelnigg, W. Koch and P. Pulay, *Angew. Chem.* **101**, 1063 (1989); *Angew. Chem., Int. Ed. Engl.* **28**, 1042 (1989).
45. (a) S. Sieber, P. Buzek, P. v. R. Schleyer, W. Koch and J. W. Carneiro, *J. Am. Chem. Soc.* **115**, 259 (1993); (b) Ref. 1g; (c) Ref. 26.
46. (a) W. Koch, B. Liu and P. v. R. Schleyer, *J. Am. Chem. Soc.* **111**, 3479 (1989); (b) W. Koch, B. Liu and D. J. Defrees, *J. Am. Chem. Soc.* **110**, 7325 (1988); (c) Refs 44 a, e, g.
47. G. A. Olah and D. J. Donovan, *J. Am. Chem. Soc.* **100**, 5163 (1978).
48. A. M. Orendt, J. C. Facelli, D. M. Grant, J. Michl, F. J. Walker, W. P. Dailey, S. T. Waddell, K. B. Wiberg, M. Schindler and W. Kutzelnigg, *Theor. Chim. Acta* **68**, 241 (1985).
49. M. Pilz, J. Allwohn, M. Bühl, P. v. R. Schleyer and A. Berndt, *Z. Natuforsch., Teil B* **46**, 1085 (1991).
50. R. Ditchfield, *Mol. Phys.* **27** 789 (1974).
51. (a) D. Cremer, E. Kraka, *Angew. Chem., Int. Ed. Engl.* **23**, 627 (1984); (b) D. Cremer and E. Kraka, *Croat. Chem. Acta* **57**, 1259 (1984).
52. (a) R. F. W. Bader, T. S. Slee, D. Cremer and E. Kraka, *J. Am. Chem Soc.* **105**, 5061 (1983); (b) for a recent application on carbocations, see R. F. W. Bader and K. E. Laidig, *J. Mol. Struct. (Theochem)* **261**, 1 (1992).